Magnetic Resonance in Medicine 42:591–598 (1999)

Vascular Filters of Functional MRI: Spatial Localization Using BOLD and CBV Contrast

Joseph B. Mandeville[1,2]* and John J.A. Marota[1,3]

The spatial distributions of functional activation of rat somatosensory cortex by forepaw stimulation were quantitatively compared using blood oxygen level dependent (BOLD) signal and signal weighted by cerebral blood volume (CBV). The BOLD contrast to noise (CNR) distribution showed a significant dorsal shift with respect to the CBV method at fields strengths of 2 T (0.69 ± 0.09 mm) and 4.7 T (0.44 ± 0.15 mm). These shifts were attributed to the gradient of resting state blood volume across somatosensory cortex and the different CNR characteristics of the two image methods. The underlying principles suggest that the CBV method has a more uniform sensitivity to percent changes in functional indicators (blood volume or deoxygenated hemoglobin) across regions of variable resting state CBV. Magn Reson Med 42:591–598, 1999. © **1999 Wiley-Liss, Inc.**

Key words: MRI; BOLD; CBV, iron oxide; forepaw

All imaging modalities that infer changes in neuronal activity from vascular measurements produce functional maps that have passed through a vascular filter; that is, the regional sensitivity of the modality for detecting functional changes depends upon the vascular baseline state. Since functional brain maps are generally derived from statistical tests for each image voxel, spatial localization is determined from the contrast to noise ratio (CNR) of the imaging modality. It is well known that the CNR of blood oxygen level dependent (BOLD) functional magnetic resonance imaging (fMRI) depends strongly on the resting state blood volume fraction (1,2). For this reason, BOLD signal changes in gray matter will be larger than those in white matter for the same percent change in the concentration of deoxygenated hemoglobin ([dHb]). Furthermore, large BOLD signal changes are often associated with large veins. This latter issue has been referred to as the ''brain versus vein'' ambiguity.

Exogenous intravascular contrast agents with long blood half lives have provided a sensitive new functional imaging tool for animal studies of sensory stimuli (3–7), respiratory challenges (3,8–10), pharmacological challenges (11), and pathology (9,10,12). Injection of a large dose of agent modifies many characteristics of T_2*-weighted fMRI. First, changes in MRI signal reflect changes in cerebral blood volume (CBV), rather than [dHb] as in BOLD imaging. Second, the magnitude of CNR is increased relative to BOLD imaging by a large factor at typical magnetic field strengths (3,5). Finally, the CNR of CBV fMRI depends primarily upon the *percent* change in CBV (3,5), while the CNR of BOLD fMRI depends upon the *absolute* change in [dHb].

The consequences of this last point are the focus of this report. We first describe the theoretical difference between BOLD fMRI and CBV fMRI in terms of the dependence of CNR on resting state CBV. We then investigate whether local variations in the blood volume fraction produce measurable differences in the macroscopic spatial localization of changes in brain activity as inferred by the two functional imaging methods. Rat forepaw stimulation provides an ideal model for this task, since neuronal activation is localized in somatosensory cortex, which exhibits a large blood volume gradient from the inner to the outer cortical layers (13). Finally, we quantitatively compare the spatial distributions of percent changes in CBV and [dHb], and we discuss the more general implications of the respective ''vascular filters'' for BOLD and CBV fMRI.

MATERIALS AND METHODS

Electrical Stimulation of Rat Forepaw

This report describes a quantitative spatial analysis of data that has been presented previously in different contexts (3,6). A detailed description of the experimental methods can be found in those papers.

Briefly, electrical stimuli were applied to the forepaws of rats anesthetized with α-chloralose, paralyzed with pancuronium, and mechanically ventilated. Data from three different stimulation paradigms were analyzed to determine the first and second moments of functional CNR for each contrast method. In the first paradigm (2 T: six paws, four rats; 4.7 T: six paws, five rats), the durations of stimuli and rest were 30 and 150 sec. In the second paradigm (2 T: two paws, one rat; 4.7 T: three paws, two rats), the durations of stimuli and rest were 120 and 180 sec. In the third paradigm (2 T: four paws, two rats), the durations of stimuli and rest were 6 and 54 sec. We have not observed any difference in the attenuation characteristics with repeated electrical stimulations for CBV imaging relative to either BOLD imaging or CBF measurements by laser doppler flowmetry.

Data were collected at both 2.0 T and 4.7 T. A repetition time of 3 sec was used for all stimuli of 30 and 120 sec duration, and a repetition time of 350 msec was used for the 6 sec stimuli. Gradient echo times of 25 msec were used. The slice thickness during these studies was typically 1 mm, and spatial resolution in the image plane was 0.8 mm in each dimension; all images were interpolated by padding the data with zeroes prior to Fourier transformation. In each experiment, functional imaging data using

[1]NMR Center, Massachusetts General Hospital, Charlestown, Massachusetts.

[2]Department of Radiology, Massachusetts General Hospital, Boston, Massachusetts.

[3]Department of Anesthesia and Critical Care, Massachusetts General Hospital, Boston, Massachusetts.

Grant sponsor: National Institutes of Health; Grant numbers: DA00384; DA09467.

*Correspondence to: Joseph B. Mandeville, Ph.D., Massachusetts General Hospital, NMR Center, Room 2301, Building 149, 13th Street, Charlestown, MA 02129. E-mail: jbm@nmr.mgh.harvard.edu

Received 24 February 1999; revised 7 May 1999; accepted 16 June 1999.

BOLD and CBV contrast were sequentially acquired in the same animal using identical stimulation paradigms and imaging protocols. To weight MRI signal by CBV rather than the concentration of deoxygenated hemoglobin, a monocrystalline iron oxide nanocolloid (MION) was injected intravenously at an iron dose of 12 mg/kg.

Contrast to Noise Ratio: Theory

It is convenient to consider CNR at spatial location **r** and time *t* as the product of the signal to noise ratio (SNR) before injection of contrast agent, a vascular weighting function (W), and a term that depends upon functional changes (Φ) but is independent of baseline physiology:

$$\mathrm{CNR}(\mathbf{r}, t) = \mathrm{SNR}(\mathbf{r})W(\mathbf{r})\Phi(\mathbf{r}, t). \quad [1]$$

Expressions for the CNR of BOLD fMRI and CBV fMRI are given by Eqs. [A2] and [A5] in the Appendix. By comparison, the functions of Eq. [1] can be written as

$$W_{BOLD}(\mathbf{r}) \approx Kv(\mathbf{r}), \qquad \Phi_{BOLD}(\mathbf{r}, t) \approx -\Delta[\mathrm{dHb}](\mathbf{r}, t)/[\mathrm{dHb}](\mathbf{r}, 0)$$

$$W_{CBV}(\mathbf{r}) \approx v(\mathbf{r})e^{-v(\mathbf{r})}, \quad \Phi_{CBV}(\mathbf{r}, t) \approx -\Delta V(\mathbf{r}, t)/V(\mathbf{r}, 0), \quad [2]$$

where V is the blood volume fraction, $v(\mathbf{r}) = V(\mathbf{r})/V(\mathbf{r}_0)$ is the resting state blood volume relative to some position $\mathbf{r}_0$, and $K = T_E R_2^{*(BOLD)}(\mathbf{r}, 0)$ is a constant. We have previously measured the BOLD resting state relaxation rate ($R_2^{*(BOLD)}$) in rat somatosensory cortex (14).

The weighting functions for these fMRI methods differ due to injection of contrast agent, which reduces SNR proportional to a decreasing exponential of relative blood volume. Figure 1 graphically depicts weighting functions versus relative blood volume, which can be defined experimentally in terms of the ratio of signal intensities before (S_{BOLD}) and after (S_{CBV}) injection of contrast agent as $v(\mathbf{r}) = -\ln(S_{CBV}/S_{BOLD})$. CNR for CBV-fMRI is optimal at a location where signal is reduced by exogenous contrast agent to 1/e of the pre-injection value so that $v(\mathbf{r}_0) = -\ln(S_{CBV}/S_{BOLD}) = 1$. In the figure, two curves are shown for the vascular weight of CBV fMRI; the dashed line indicates the effect of BOLD contamination in the predominantly CBV-weighted signal, as calculated in Eq. [A6].

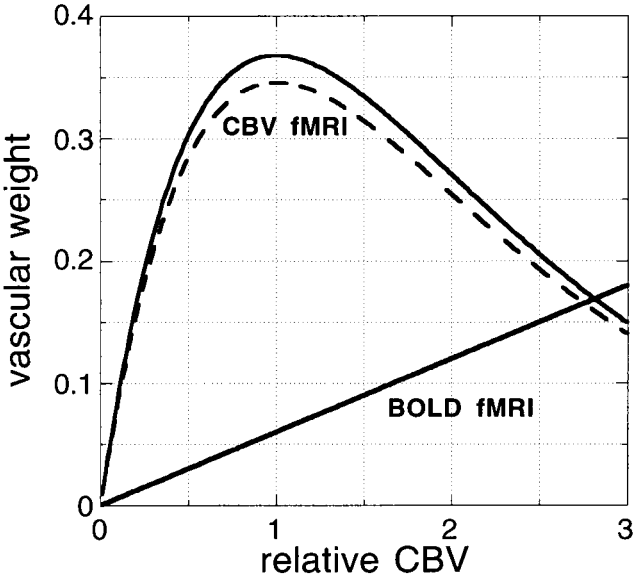

FIG. 1. Theoretical vascular weights for BOLD and CBV fMRI at 2 T versus the resting state blood volume fraction as given in Eq. [2] and the Appendix. The dashed line shows the calculated vascular weight for CBV fMRI after including the BOLD effect (Eq. [A6]). The essential point is that BOLD fMRI linearly amplifies CNR by resting state CBV, whereas CBV fMRI is much less sensitive to resting blood volume when an appropriate dose of contrast agent is used.

As depicted in the figure, the dependence of CNR on resting state blood volume is much stronger for BOLD fMRI than for CBV fMRI, which is insensitive to small changes in resting state CBV about the point v = 1 and decreases the CNR weighting when the magnitude of resting state CBV deviates in either direction from this value. In contrast, BOLD CNR changes with a roughly linear dependence on resting state blood volume, exacerbating the ''brain versus vein'' ambiguity due to CNR amplification in large veins.

Contrast to Noise Ratio: Analysis

A comparison of the CNR profiles obtained by fMRI using BOLD and CBV contrast was made using both image-based analyses and a dorsal-ventral projection analysis through the medial-lateral centroid of BOLD activation in somatosensory cortex. In each case, Student's pooled *t* test was applied to the temporal data for each voxel to compare MRI signal between stimulated and non-stimulated states. The *t* statistic, which is defined as the difference of the means (contrast) divided by the standard error of the difference of the means (noise), was used as the measure of CNR. Prior to averaging data across individual animals for each method, the CNR at the centroid of activation for each method was normalized. This step avoided large responses in individual rats from biasing average results and also circumvented the necessity of adjusting thresholds to account for the larger magnitude of CBV CNR relative to BOLD CNR.

An image-based analysis was performed in which the first and second moments and the skewness of CNR distributions for BOLD and CBV fMRI were compared in the dorsal-ventral and medial-lateral directions. To reduce error from voxels far outside somatosensory cortex, all calculations were restricted within an image overlay that fully covered unilateral forepaw somatosensory cortex in a given slice and was at least a factor of two larger than this area in each dimension. First moments were calculated as $\bar{x} = \Sigma_i \mathrm{CNR}_i x_i / \Sigma_i \mathrm{CNR}_i$, where *x* is the image coordinate and the sum is over the number of voxels. Second moments were calculated as $\sigma_x = \sqrt{\Sigma_i \mathrm{CNR}_i (x_i - \bar{x})/\Sigma_i \mathrm{CNR}_i}$. Although the expression for the second moment is valid for any distribution, second moments were reported as full width half maximum values (FWHM = 2.35σ), since CNR distributions exhibited an approximate Gaussian shape at the resolution of this study. The first moments of CNR distributions for BOLD and CBV fMRI were compared in each dimension using a paired *t* statistic to test the hypothesis that the centroids of activation were the same using the two methods. Second moments were compared using a pooled *t* statistic.

For direct visualization, average images of functional activation for BOLD and CBV fMRI were computed in a single slice in three rats at 2 T for which the image

resolutions and fields of view were consistent. Multi-slice functional images were manually registered to enable averaging of both the images and the overlying functional maps.

A dorsal-ventral projection analysis was also performed. For each rat, projections through the medial-lateral centroid of BOLD activation, as determined by the image-based analysis above, were obtained for 1) BOLD CNR, 2) CBV CNR, and 3) resting state rCBV. In most cases, projections from two adjacent image planes were averaged. The dorsal-ventral origin of each projection was defined as the centroid of activation according to CBV fMRI, and all projections were then averaged using this axis convention. The first and second moments of each CNR distribution and the skewness, $\Sigma_i CNR_i[x_i - x/\sigma]^3/\Sigma_i CNR_i$, were computed and compared between imaging methods. The vascular weighting functions of Eq. [2] were calculated, and the CNR distributions for BOLD and CBV fMRI were compared before and after dividing by the vascular weighting functions.

RESULTS

Image-Based Analysis

Figure 2 shows average CNR distributions for BOLD fMRI (left) and CBV fMRI (right) in a subset of the data at 2 T (three rats, six forepaws). Functional maps for both forepaws are shown together for the sake of brevity; we detected no activation of somatosensory cortex ipsilateral to the stimulated forepaw in any animal using either method. A dorsal shift of the centroids of BOLD CNR relative to CBV CNR is apparent in the figure.

In the comparison of the CNR distributions for BOLD and CBV fMRI, neither the relative positions of the centroids nor the widths of the distributions were found to depend upon the duration of stimulation (pooled *t* tests; $P > 0.05$); therefore, data from the three stimulation paradigms were averaged. The average location of the BOLD centroid of functional activation was not the same as CBV fMRI in either the dorsal-ventral or medial-lateral directions at either magnetic field strength. With respect to the centroid of CNR determined by CBV fMRI, the centroid of BOLD CNR was shifted predominantly toward the outer layer of cortex (2 T: 0.69 ± 0.09 mm, $P < 10^{-4}$; 4.7 T: 0.44 ± 0.15 mm, $P < 0.05$) but was also shifted medially (2 T: 0.26 ± 0.05 mm, $P < 10^{-3}$; 4.7 T: 0.26 ± 0.09 mm, $P < 0.05$). The FWHM of the CNR distributions for BOLD and CBV fMRI were not statistically different in either direction ($P > 0.05$).

Projection Analysis

Dorsal-ventral projections through the medial-lateral centroids of BOLD activation were computed and averaged across animals at both field strengths. Table 1 shows results in individual animals at both field strengths. Note that the centroid of BOLD CNR was shifted in the dorsal direction with respect to the centroid of CNR for CBV fMRI in every case at both field strengths.

Figure 3a shows normalized CNR distributions for BOLD and CBV fMRI at 2 and 4.7 T after averaging across animals and stimulation paradigms. The FWHM of the BOLD (2 T: 1.50 ± 0.03 mm; 4.7 T: 1.48 ± 0.10 mm) and CBV distributions (2 T: 1.41 ± 0.03 mm; 4.7 T: 1.43 ± 0.09 mm) did not depend upon either the imaging method or the field strength ($P > 0.05$; pooled *t* tests). However, the highly significant shift between activation centroids of the two methods was evident, as noted in the image-based analysis. While the shift at 4.7 T (0.45 ± 0.12 mm, $P < 10^{-2}$) was slightly smaller than the shift at 2 T (0.67 ± 0.09 mm, $P < 10^{-4}$), this trend was not significant ($P > 0.05$). Finally, the skewness of the distributions of BOLD CNR (2 T: -0.19 ± 0.05; 4.7 T: -0.23 ± 0.10) and CBV CNR (2 T: -0.08 ± 0.06; 4.7 T: -0.24 ± 0.05) were not statistically different ($P > 0.05$).

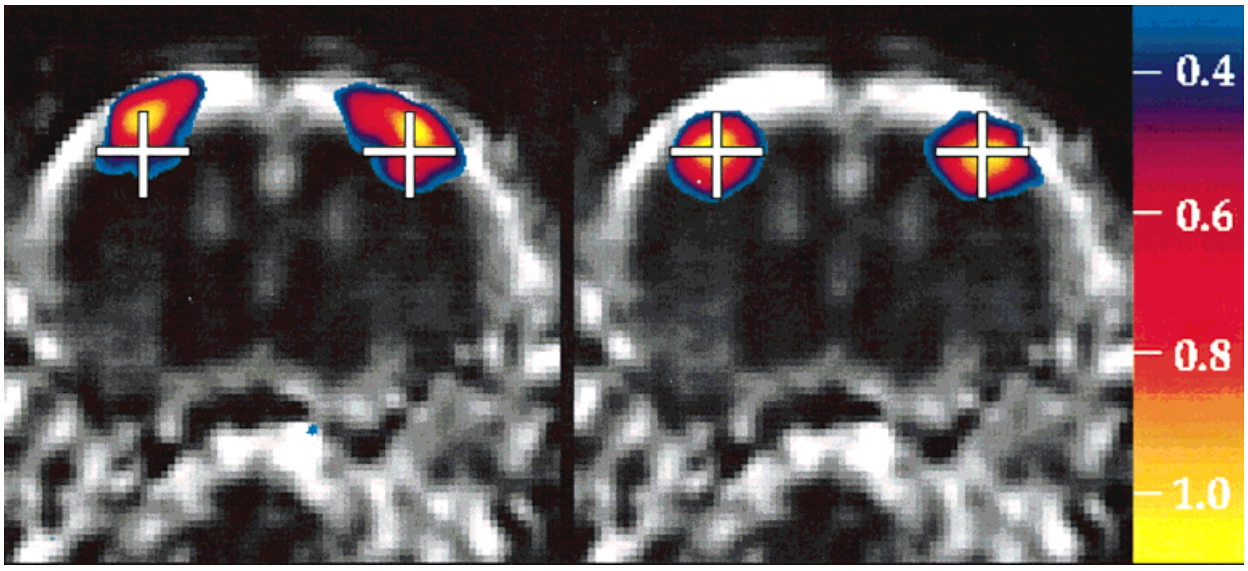

FIG. 2. An average image (n = 3 rats) of the relative blood volume fraction in rat brain calculated as the negative log ratio of the signal attenuation produced by injection of MION contrast agent. Percent CNR as determined by BOLD fMRI (left) shows a dorsal shift with respect to CBV fMRI (right) as a result of BOLD amplification at high blood volume fractions. Crosses are located consistently in the two images.

Table 1
Results From Individual Rats at Both Field Strengths*

2 T				4.7 T			
Rat paw	Centroid shift (mm)	BOLD FWHM (mm)	CBV FWHM (mm)	Rat paw	Centroid shift (mm)	BOLD FWHM (mm)	CBV FWHM (mm)
1a[a]	0.59	1.57	1.41	1[b]	1.04	1.47	1.29
1b[a]	1.07	1.39	1.20	2[b]	0.92	1.85	1.75
2[b]	0.54	1.64	1.42	3[b]	0.14	1.34	1.42
3[b]	0.76	1.55	1.61	4[b]	0.76	1.96	1.89
4a[a]	0.58	1.43	1.38	4[c]	0.35	1.62	1.56
4a[b]	0.27	1.43	1.34	5a[b]	0.11	1.20	1.28
4b[a]	0.33	1.54	1.38	5a[c]	0.06	1.61	1.33
4b[b]	0.39	1.62	1.35	5b[b]	0.34	1.20	1.23
5a[b]	1.36	1.47	1.50	5b[c]	0.31	1.06	1.10
5a[c]	1.02	1.60	1.46				
5b[b]	0.56	1.35	1.52				
5b[c]	0.62	1.36	1.39				
Mean ± SEM	0.67 ± 0.09	1.50 ± 0.03	1.41 ± 0.03		0.45 ± 0.12	1.48 ± 0.10	1.43 ± 0.09

*In every rat, the centroid of CNR distribution for BOLD fMRI exhibited a dorsal shift with respect to the centroid using CBV fMRI. The widths of the two distributions were found to be the same.
[a]Paradigm: 6 sec of stimulation followed by 54 sec of rest.
[b]Paradigm: 30 sec of stimulation followed by 150 sec of rest.
[c]Paradigm: 120 sec of stimulation followed by 180 sec of rest.

The vascular weights of Eq. [2] are shown in Fig. 3b. The relative blood volume fraction, calculated as the negative log of the ratio of signal intensities after and before injection of MION contrast agent, was largest on the outer layers of cortex on the dorsal side of the activation centroids; a steep blood volume gradient extended across the activated region of somatosensory cortex. This BOLD ''amplification factor'' of functional sensitivity was about a factor of 2 larger in cortex than striatum. In contrast, the calculated vascular weight for CBV fMRI showed much more uniformity; variations were not larger than 20% across parenchymal tissue.

Figure 3c shows the effect of dividing the activation distributions by the respective vascular weights of Fig. 3b and renormalizing the distributions. Approximately half of the shift between centroids was removed by this calculation (2 T: 0.31 ± 0.16 mm, $P < 0.01$; 4.7 T: 0.29 ± 0.10 mm, $P < 0.05$), but the remaining shift at each field strength was still statistically significant. This result suggested that the assumptions employed in Eq. [2] and the Appendix may not produce precise representations of the vascular weights. In fact, it was possible to completely remove the observed shift by slight modifications of either (or both) of the weighting functions of Eq. [2]. For instance, Fig 4 shows a slightly superlinear BOLD vascular weight and a weighting function for CBV fMRI that peaks at a relative volume fraction below 1. After dividing the measured CNR distributions by these vascular weights, the resulting distributions were found to exhibit no statistical differences in either centroid position or width at either field strength (e.g., Fig. 4b).

DISCUSSION

Because locations of brain activation using noninvasive imaging are determined from statistical tests on temporal data, foci of activity are ultimately derived from CNR distributions. In this study, a striking systematic shift was observed between CNR distributions of functional activation in rat somatosensory cortex using two different imaging methods: BOLD and CBV-weighted fMRI. Our analysis showed that resting state CBV amplifies CNR in a different manner for the two methods, and this effect must be taken into account before assigning a physiological significance to the shift of ''functional activation.'' In fact, the analysis showed that a shift in the observed direction *must* result if percent changes in blood volume and deoxyhemoglobin concentration are spatially co-localized and activation occurs on a blood volume gradient, as in rat somatosensory cortex. Furthermore, the underlying principles suggest that the functional sensitivity of CBV fMRI is more regionally uniform than that of the BOLD method; this characteristic has general implications for comparisons of regional magnitudes and vascular artifacts between the two methods.

Spatial Localization

The essential difference between spatial localization of brain function using these methods is that BOLD fMRI measures *absolute* changes in the concentration of deoxygenated hemoglobin, while CBV fMRI measures *percent* changes in blood volume when a sufficient dose of contrast agent is used. Therefore, a gradient of resting state CBV (and presumably also [dHb]) caused a highly significant shift between measured CNR centroids using BOLD and CBV contrast. The spatial extents of activation, as measured by the second moment of the CNR distributions, were not found to be statistically different.

Resting state blood volume was assumed to be the single most important determinant of regional functional sensitivity, and this assumption could account for the observed shift in activation centroids within the accuracy of our knowledge of the respective vascular weighting functions. The BOLD vascular weight was formulated as a roughly linear function of the blood volume fraction under the presumption of regional invariance in the resting state venous blood concentration of deoxygenated hemoglobin, which is determined by the ratio of oxygen utilization to

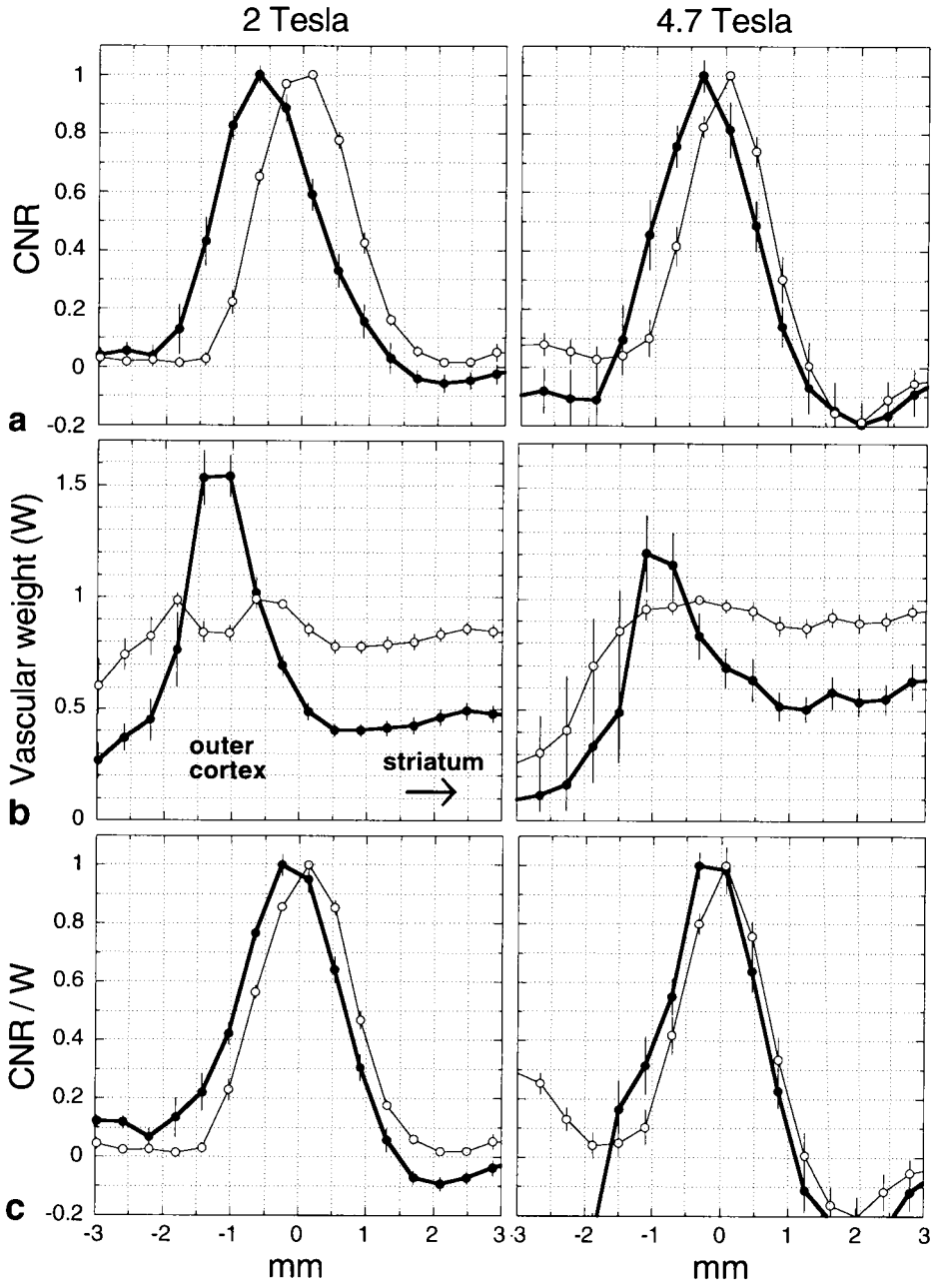

FIG. 3. Dorsal-ventral projections through somatosensory cortex from functional images obtained at field strengths of 2 T (left) and 4.7 T (right). **a:** Average normalized CNR of BOLD (closed circles) and CBV (open circles) functional imaging. **b:** Corresponding vascular weights proportional to those defined in Eq. [2]. Closed circles show relative blood volume calculated from the negative log ratio of signals before and after injection of contrast agent (v in Eq. [2]), and open circles show a gamma function of relative blood volume with maxima scaled to unity. **c:** Division by the vascular weights of Eq. [2] removed about half of the observed shift between activation centroids.

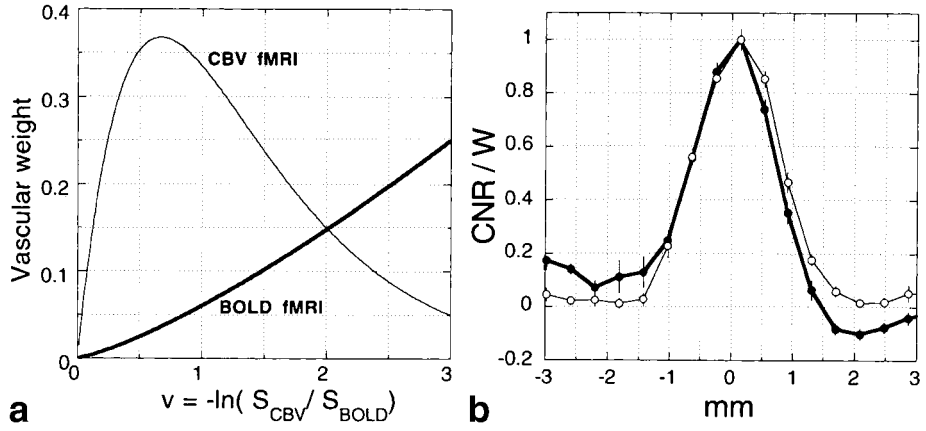

FIG. 4. After correcting activation centroids at 2 T using slightly modified forms of the vascular weighting functions, activation centroids were found to co-localize. **a:** Modified vascular weighting functions. **b:** CNR divided by vascular weights for fMRI weighted by BOLD signal (closed circles) and CBV (open circles).

blood flow. Positron emission tomography experiments have consistently found a tight linear regional coupling between oxygen utilization and blood flow in the resting state at coarse spatial resolution (15–17). In the case of CBV fMRI, the vascular weight was shown to take the form of a gamma function in the relative blood volume fraction.

The vascular weighting functions of Eq. [2] make several simplifying assumptions that are described in the Appendix and may not be strictly accurate. Although it was assumed that the BOLD relaxation rate is linearly proportional to resting state CBV (1,18), this is difficult to validate experimentally. Similarly, it is possible that the CNR for CBV fMRI may be optimized at smaller values of the product of CBV and agent dose than shown in Fig. 1. For instance, if noise becomes correlated with $-\ln(S_{CBV}/S_{BOLD})$ at sufficiently large values, the maximum of the weighting function would be shifted to lower values of blood volume and dose. Using the theoretical vascular weights in the Appendix did not account fully for the observed centroid shifts. It is possible that changes in blood volume and dexoxyhemoglobin do not perfectly co-localize due to effects like draining veins in BOLD signal. However, additional studies are required to further refine the accuracy of the vascular weighting functions for each method.

We observed a slightly smaller shift between activation centroids in the data acquired at 4.7 T relative to the 2 T data. At very high magnetic field strengths, the magnetic susceptibility difference between paramagnetic deoxyhemoglobin and surrounding tissue will increase and should therefore make the CNR characteristics of BOLD signal more like that of an iron oxide. Indeed, the ratio of MR-visible blood volume between the outer cortical layers and the striatum was reduced at 4.7 T relative to 2 T. Although this may result from signal loss around large cortical vessels due to stronger blood magnetization at a higher magnetic field, it might also be due to larger macroscopic field gradients arising at the air-tissue interface on the surface of the head. In either case, the effect of field strength on the shift of CNR centroids was modest.

Implications for Regional Sensitivity

The small shift between activation centroids illustrates a larger point: BOLD fMRI and CBV fMRI have very different regional sensitivities to underlying functional changes. For instance, Fig. 3b predicts that CBV fMRI will have roughly equal sensitivity to an equal percent change in blood volume in the striatum and cortex, while BOLD fMRI will be much more sensitive to cortical than striatal activation for equal percent changes in [dHb]. This prediction can be tested using functional challenges that produce both cortical and subcortical activation, such as administration of cocaine (11); our preliminary results support the idea that BOLD signal amplifies cortical relative to subcortical CNR in a comparison with CBV fMRI.

A useful practical feature of brain mapping by CBV fMRI is that CNR can be optimized for ''parenchyma,'' which exhibits a small variation in resting state CBV relative to the variation between parenchyma and large blood vessels. For instance, the blood volume fraction of gray matter is larger than that of white matter by about a factor of 2 in human brain (19–21), but blood volume can vary by an order of magnitude between image pixels with and without large veins. While BOLD fMRI is very sensitive to large veins that can be distal to the site of neuronal activation, CBV fMRI will show less sensitivity to large blood vessels than parenchymal tissue, because the vascular weighting function penalizes very high blood volume fractions (Fig. 1).

CBV fMRI is now an attractive functional imaging alternative to the BOLD method in animal model applications due to the large increase in functional sensitivity, higher uniformity of functional sensitivity, and suppression of large vessel artifacts. These advantages offer intriguing possibilities for human clinical studies if suitable contrast agents obtain human approval.

APPENDIX

CNR for BOLD fMRI

Functional CNR, which is defined as the ratio of signal change to noise, is the product of SNR in the baseline state times the fractional signal change during functional brain activation. Assuming monoexponential signal decay, the CNR for BOLD imaging can be written as $CNR_{BOLD}(\mathbf{r}, t) = SNR(\mathbf{r})\ (e^{-T_E\Delta R_2^*(\mathbf{r},t)} - 1)$, where $SNR(\mathbf{r})$ is the signal to noise ratio at vector location $\mathbf{r}$, T_E is the echo time, and $\Delta R_2^*(\mathbf{r},t)$ is the change in transverse relaxation rate of BOLD signal at location $\mathbf{r}$ and time t. For small MRI signal changes, the exponent can be expanded to give $CNR_{BOLD}(\mathbf{r}, t) \approx -SNR(\mathbf{r})\ T_E\Delta R_2^*(\mathbf{r}, t)$. This result can be rewritten in terms of the percent change in the BOLD relaxation and the absolute value of the BOLD relaxation rate with respect to any specific spatial location at $\mathbf{r_0}$:

$$CNR_{BOLD}(\mathbf{r}, t) \approx -SNR(\mathbf{r})T_E R_2^{*(BOLD)}(\mathbf{r}, 0) \cdot \frac{R_2^{*(BOLD)}(\mathbf{r}, 0)}{R_2^{*(BOLD)}(\mathbf{r}_0, 0)} \frac{\Delta R_2^*(\mathbf{r}, t)}{R_2^{*(BOLD)}(\mathbf{r}, 0)}. \quad [A1]$$

The BOLD part of the transverse relaxation can be written as $R_2^{*(BOLD)} = KV(M/F)^{\beta}$ (14), where K and B are constants and V, F, and M denote cerebral blood volume, cerebral blood flow (CBF), and the cerebral metabolic rate of oxygen utilization ($CMRO_2$), respectively. Measurements by positron emission tomography in humans (15–17) have consistently shown a tight regional linear relationship between resting state values of CBF and $CMRO_2$. Therefore, the regional variation of resting state deoxygenated hemoglobin should closely approximate the regional variation in the blood volume fraction. Writing relative regional blood volume with respect to the value at position $\mathbf{r_0}$ as $v(\mathbf{r}) = V(\mathbf{r}, 0)/V(\mathbf{r}, 0)$ and assuming CBF-$CMRO_2$ coupling in the resting state,

$$CNR_{BOLD}(\mathbf{r}, t) \approx -SNR(\mathbf{r})T_E R_2^{*(BOLD)}(\mathbf{r}_0, 0)\ v(\mathbf{r}) \frac{\Delta R_2^*(\mathbf{r}, t)}{R_2^{*(BOLD)}(\mathbf{r}, 0)}. \quad [A2]$$

Eq. [A2] expresses the percent change in BOLD signal in terms that are essentially identical to the form proposed by Ogawa et al. (1), except that a coupling between resting state CBF and $CMRO_2$ has been enforced.

CNR for CBV fMRI

The general expression for the CNR of CBV fMRI using simplifying assumptions has been presented previously (3).

$$CNR_{CBV}(\mathbf{r}, t) = SNR(\mathbf{r})e^{-T_E KV(\mathbf{r},0)}(e^{-T_e K\Delta V(\mathbf{r},t)} - 1), \quad [A3]$$

where SNR(**r**) is the SNR prior to injection of contrast agent, V(**r**,0) is the blood volume fraction of the baseline state prior to the functional challenge, ΔV(**r**,t) is the change in blood volume fraction during the functional challenge, and Kis a constant that depends upon the dose of contrast agent. CNR depends upon the product of contrast agent dose and resting state blood volume and is maximized at location $\mathbf{r_0}$ for any fixed echo time by injecting a quantity of contrast agent such that the baseline SNR is reduced to approximately 1/e of the value prior to injection (3); in this case, $T_E KV(\mathbf{r}_0, 0) = 1$. Defining the relative resting state blood volume fraction (v(**r**)) as before, the two exponents in Eq. [A3] can be rewritten as

$$T_E KV(\mathbf{r}, 0) = T_E KV(\mathbf{r}_0, 0)V(\mathbf{r}, 0)/V(\mathbf{r}_0, 0)$$

$$= V(\mathbf{r}, 0)/V(\mathbf{r}_0, 0) = v(\mathbf{r})$$

$$T_E K\Delta V(\mathbf{r}, t) = T_E KV(\mathbf{r}_0, 0)V(\mathbf{r}, 0)/V(\mathbf{r}_0, 0)$$

$$\cdot \Delta V(\mathbf{r}, t)/V(\mathbf{r}_0, 0) = v(\mathbf{r})\Delta V(\mathbf{r}, t)/V(\mathbf{r}, 0). \quad [A4]$$

By replacing the exponents in Eq. [A3] with the expressions on the right hand side of Eqs. [A4] and expanding the exponential for small relative volume changes, CNR can be written as

$$CNR(\mathbf{r}, t) \approx -SNR(\mathbf{r})v(\mathbf{r})e^{-v(\mathbf{r})}\Delta V(\mathbf{r}, t)/V(\mathbf{r}, 0). \quad [A5]$$

Note that the reference point ($\mathbf{r_0}$) for relative blood volume (v) is determined experimentally by finding a location where the signal intensity drops by e^{-1} due to exogenous contrast agent. In our studies, this location occurred near the peaks of functional activation (Fig. 3b).

CNR for CBV fMRI Including the BOLD Effect

Eq. [A5] can be modified to include BOLD contamination in the CBV-weighted signal. Assuming that relaxation rates due to BOLD and exogenous contrast agent are additive, we can expand exponentials as done above and arrive at the following expression:

$$CNR(\mathbf{r}, t) \approx -SNR(\mathbf{r})\Delta V(\mathbf{r}, t)/V(\mathbf{r}, 0)e^{-Dv(\mathbf{r})}$$

$$\cdot (Dv(\mathbf{r}) - T_E R_2^{*(BOLD)}(\mathbf{r}_0, 0)A_C v(\mathbf{r})), \quad [A6]$$

where A_C is a coupling constant relating percent changes in blood volume and deoxyhemoglobin concentration ([dHb]) as $\Delta R_2/R_2^{*(BOLD)} = -A_C\ \Delta V/V$ ($\approx\Delta$[dHb]/[dHb]), and $D = T_E KV(\mathbf{r}_0, 0)$ is a function of the dose of iron oxide contrast agent. For signal intensities before (S_{BOLD}) and after (S_{CBV}) injection of contrast agent, $Dv(\mathbf{r}) = -\ln(S_{CBV}/S_{BOLD})$. Eq. [A6] predicts the dependence of CNR versus relative dose (D) at any point $\mathbf{r_0}$ where v(**r**) = 1, and it also predicts the dependence of CNR on blood volume (v) relative to the point $\mathbf{r_0}$ for which $D = -\ln(S_{CBV}/S_{BOLD}) = 1$.

Our previous measurements have shown that $A_C \simeq 1$ and $R_2^{*(BOLD)} \simeq 2.4\ sec^{-1}$ in somatosensory cortex at 2 T (14). Therefore, Eq. [A6] predicts that CBV fMRI with a 25 msec echo time will increase CNR at D = 1 by a factor of about 5.8 relative to BOLD fMRI (D = 0), which is in complete agreement with our report of CNR magnitudes at 2 T (3). Fig. 1 shows that the BOLD effect is only a very small influence on CBV fMRI when enough contrast agent is used to drop baseline signal to e^{-1} of the value before injection (i.e., D = 1).

REFERENCES

1. Ogawa S, Lee RM, Barrere B. The sensitivity of magnetic resonance image signals of a rat brain to changes in the cerebral venous blood oxygenation. Magn Reson Med 1993;29:205–210.
2. Bandettini PA, Wong EC. A hypercapnia-based normalization method for improved spatial localization of human brain activation with fMRI. NMR Biomed 1997;10:197–203.
3. Mandeville JB, Marota JJA, Kosofsky BE, Keltner JR, Weissleder R, Rosen BR, Weisskoff RM. Dynamic functional imaging of relative cerebral blood volume during rat forepaw stimulation. Magn Reson Med 1998;39:615–624.
4. van Bruggen N, Busch E, Palmer JT, Williams SP, de Crespigny AJ. High-resolution functional magnetic resonance imaging of the rat brain: mapping changes in cerebral blood volume using iron oxide contrast media. J Cereb Blood Flow Metab 1998;18:1178-–183.
5. Kennan RP, Scanley BE, Innis RB, Gore JC. Physiological basis for BOLD MR signal changes due to neuronal stimulation: separation of blood volume and magnetic susceptibility effects. Magn Reson Med 1998;40: 840–846.
6. Marota JJA, Ayata C, Moskowitz MA, Weisskoff RM, Rosen BR, Mandeville JB. Investigation of the early response to rat forepaw stimulation. Magn Reson Med 1999;41:247–252.
7. Mandeville JB, Marota JJA, Ayata C, Zaharchuk G, Moskowitz MA, Rosen BR, Weisskoff RM. Evidence of a cerebrovascular post-arteriole windkessel with delayed compliance. J Cereb Blood Flow Metab 1999;19:679–689.
8. Kennan RP, Scanley BE, Gore JC. Physiologic basis for BOLD MR signal changes due to hypoxia/hyperoxia: separation of blood volume and magnetic susceptibility effects. Magn Reson Med 1997;37:953–956.
9. Payen J-F, Vath A, Koenigsberg B, Bourlier V, Decorps M. Regional cerebral plasma volume response to carbon dioxide using magnetic resonance imaging. anesthesiology 1998;88:984–992.
10. Zaharchuk G, Bogdanov Jr. AA, Marota JJA, Shimizu-Sasamata M, Weisskoff RM, Kwong KK, Jenkins BG, Weissleder R, Rosen BR. Continuous assessment of perfusion by tagging including volume and water extraction (CAPTIVE): a steady-state contrast agent technique for measuring blood flow, relative blood volume fraction, and the water extraction fraction. Magn Reson Med 1998;40:666–678.
11. Marota JJA, Mandeville JB, Ayata C, Kosofsky B, Weissleder R, Hyman S, Moskowitz M, Weisskoff RM, Rosen BR. Activation of rat brain by cocaine: functional imaging with BOLD and cerebral blood volume. In: Proceedings of the International Society of Magnetic Reasonance Imaging Med, Vancouver, 1997. p 731.
12. Hamberg L, Boccalini P, Stranjalis G, Hunter G, Huang Z, Halpern E, Weisskoff R, Moskowitz M, Rosen B. Continuous assessment of relative cerebral blood volume in transient ischemia using steady state susceptibility-contrast MRI. Magn Reson Med 1996;35:168–173.
13. Hamberg LM, Hunter GJ, Halpern EF, Hoop B, Gazelle GS, Wolf GL. Quantitative high-resolution measurement of cerebrovascular physiology with slip-ring CT. Am J Neuroradiol 1996;17:639–650.
14. Mandeville JB, Marota JJA, Ayata C, Moskowitz MA, Weisskoff RM, Rosen BR. An MRI measurement of the temporal evolution of relative CMRO2 during rat forepaw stimulation. Magn Reson Med, in press.
15. Raichle ME, Grubb RL, Gado MH, Eichling JO, Ter-Pogossian MM. Correlation between regional cerebral blood flow and oxidative metabolism. In vivo studies in man. Arch Neurol 1976;33:523–526.

16. Baron JC, Rougemont D, Soussaline F, Bustany P, Crouzel C, Bousser MG, Comar D. Local interrelationships of cerebral oxygen consumption and glucose utilization in normal subjects and in ischemic stroke patients: a positron tomography study. J Cereb Blood Flow Metab 1984;4:140–149.
17. Fox PT, Raichle ME. Focal physiological uncoupling of cerebral blood flow and oxidative metabolism during somatosensory stimulation in human subjects. Proc Natl Acad Sci (USA) 1986;83:1140–1144.
18. Boxerman JL, Hamberg LM, Rosen BR, Weisskoff RM. MR contrast due to intravascular magnetic susceptibility perturbations. Magn Reson Med 1995;34:555–566.
19. Penn RD, Walser R, Ackerman L. Cerebral blood volume in man: computer analysis of a computerized brain scan. JAMA 1975;234:1154–1155.
20. Grubb RL, Raichle ME, Higgins CS, Eichling JO. Measurement of regional cerebral blood volume by emission tomography. Ann Neurol 1978;4:322–328.
21. Rosen BR, Belliveau JW, Chien D. Perfusion imaging by nuclear magnetic resonance. Magn Reson Quart 1989;5:263–281.